

Optimization of Hot-press Parameters for Plywood with Environmental Aluminophosphate Adhesive

Qihua Wei,^a Zhenzeng Wu,^{b,*} Wei Wei,^a John Tosin Aladejana,^a Kouomo Guelifack Yves,^a Dehong Li,^a Xinjun Hou,^a Xiaodong (Alice) Wang,^c and Yongqun Xie^{a,*}

An aluminophosphate adhesive was used as the binder in plywood. The hot-pressing parameters of aluminophosphate adhesive-based plywood (APPs) including hot-press temperature (A), time (B), and pressure (C) were optimized using response surface methodology. Results indicated that the hot-press temperature was the most dominant factor. The maximum bonding strength of 1.98 MPa was found with an optimal parameter of 171 °C (hot-press temperature), 7.5 min (hot-press time), and 1.0 MPa (hot-press pressure). Additionally, the chemical reaction mechanism between aluminophosphate adhesive and wood fibers was characterized by X-ray photoelectron spectroscopy (XPS). Results showed that good interaction was generated between wood fibers and adhesives through their surface functional groups. In conclusion, the optimized pressing conditions of plywood significantly improved bonding strength of APPs.

Keywords: Plywood; Hot-press parameter; Mechanical property; Optimization; Characterization

Contact information: a: Department of Material Science and Engineering, Fujian Agriculture and Forestry University, 350002, Fuzhou, Fujian, China; b: College of Ecology and Resource Engineering, Wuyi University, 354300, Wuyishan City, Fujian, China; c: Department of Wood and Forest Sciences, Laval University, G1 V 0A6, Quebec, Canada;

* Corresponding authors: zhenzeng.wu@outlook.com; fafuxieyq@aliyun.com

INTRODUCTION

Conventionally used binders in the wood industry include phenol-formaldehyde, urea-formaldehyde, and melamine-formaldehyde resins. Due to concerns about the environment and physical health, more and more researchers are paying attention to aluminophosphate adhesive (AP), which has many advantages, such as environment-friendly character and non-formaldehyde composition. However, there has been a need to study the hot-pressing parameters of AP with an essential influence on the efficiency and quality of the product. After spraying glue on the veneers with a certain pressure, temperature, and time, the adhesive began to cure and discharge some of the water; this process is called hot-pressing. Hot-pressing time refers to the time period from when the slab is compressed to a predetermined thickness to the time when the hot-pressing plate is opened. If the hot-pressing time is too short, the adhesive cannot fully cure, and the strength decreases. In this case, the moisture content of the plate is not up to standard, and it is likely that bubbles or water stains will appear. Meanwhile, incomplete removal of water from the binder can lead to steam bursting after opening the press plates. In contrast, if the hot-pressing time is too long, surface carbonization occurs. Part of the hemicellulose and lignin is degraded, which can affect the quality of the wood products (Sun *et al.* 2014). Meanwhile, the hot pressure and the mechanical properties of the product also have a

particular connection (Mei *et al.* 2012). When the pressure is low, the hot press plate cannot reach the predetermined thickness, resulting in an oversized board. If the hot pressure is too high, the hot plate can easily deform. Additionally, the pressure affects the opening and closing speed of the hot-pressing plate, which can influence the pre-curing degree of surface adhesives and the distribution of section density of the product. In turn, these changes alter the static bending strength, surface bonding strength, and internal bonding strength of the wood boards.

The preparation of wood-based boards with inorganic adhesive includes cold- and hot-pressing methods. The cold-pressing method compresses the fiber and adhesive to cure at a normal temperature. Commonly, cold-pressing methods spend more time in pressing period and need kiln drying at the end stage for the board to become fully solidified with good strength and stable performance (Zhu *et al.* 2015; Zuo *et al.* 2016; Liu *et al.* 2018), which involves many preparation steps and low production efficiency. Huang *et al.* (2018) prepared the silicon-magnesium cement bamboo particleboard with the hot-pressing method, performed at 110 °C and 9 min for the hot-pressing process. There has been a lack of published research on the hot-pressing method with an inorganic adhesive. Hot-pressing has the advantages of a short preparation period and high efficiency.

Response surface methodology (RSM) is a statistical method to obtain the best sample preparation parameters using a regression equation (Jambo *et al.* 2019; Majdi *et al.* 2019; Nayak and Vyas 2019). RSM is used to find the best response value after accounting for the variation or uncertainty of the value of the input variable (Wang and Wang 2005). RSM has the characteristics of a short test cycle, has high accuracy, and can analyze the interaction of multiple factors. RSM is widely used, such as in mechanical manufacturing (Long *et al.* 2018; Balamurugan *et al.* 2019; Song *et al.* 2019), food processing (Pérez-Francisco *et al.* 2008; Mestry *et al.* 2011; Šumić *et al.* 2016), energy utilization (Sharma *et al.* 2018), environmental management (Bahrami *et al.* 2018, 2019; Ooi *et al.* 2018), and material preparation (Sulaiman *et al.* 2018; Aghamohseni *et al.* 2019).

There appears to have been no published study that analyzes the response surface optimization of the hot-pressing process of aluminophosphate (AP) adhesive preparation. Therefore, this paper explored the optimum conditions of time, pressure, and temperature of AP adhesive used in the preparation of plywood by RSM. The reaction mechanism between aluminum phosphate adhesive and wood fiber was elucidated by analyzing the morphology, elemental distribution, and chemical bonding of plywood.

EXPERIMENTAL

Materials

Poplar veneer (10% moisture content) with a size of 30 cm × 30 cm (L × W) and a height between 0.8 and 1.0 mm, was purchased from Minhou Longhui Wood Industry Co., Ltd. (Fuzhou, China). Aluminum hydroxide (Al(OH)₃) and phosphoric acid (H₃PO₄, 85%), purchased from Tianjin Zhiyuan Chemical Reagents Factory (Tianjin, China), were used to generate the AP adhesive. In this study, the n(P)/n(Al), solid content, and viscosity of AP adhesive were 2.8, 65% w/w, and 25 to 350 mPa·s, respectively. Ferric oxide (Fe₂O₃) was purchased from Jiangsu Henglong Pigment Co., Ltd. (Xuzhou, China). The pigment was used as a curing agent.

Methods

Preparation of AP adhesive and plywood

The prepared AP adhesive and curing agent (Fe_2O_3 , 1.5% of solid AP) were lymixed first. All obtained AP was used to prepare duplicate samples of three-layer plywoods by coating 160 g/m^2 of the adhesive on each veneer layer. The AP adhesive-based plywood (AAP) was manufactured individually using various parameters. Veneers without surface defects were cut into samples sized $12 \text{ mm} \times 25 \text{ mm}$ (L×W). Then, adhesive was applied to the veneer surface. The layered veneers were put into the hot-press machine (Universal Test Press, BY302X2/15, Suzhou New Cooperation Machine Manufacturing Co. LTD, China).

Experimental design

In this study, the effect of three independent variables on the response was investigated using Box-Behnken design (BBD). The three independent variables were hot-pressing temperature (A), hot-pressing time (B), and pressure (C). The response variable was the bonding strength (BS) of plywood (Y). The specific parameters and levels are shown in Table 1. For Y, the most accepted model was selected, as suggested by the Design Expert 7.0 Trial (Static Made Easy, Minneapolis, MN, USA)

Table 1. Code and Level of Factors Chosen for the Trials

Coded Variables	Levels		
	-1	0	+1
Temperature (A/ °C)	150	165	180
Time (B/ min)	5	7	9
Pressure (C/ MPa)	0.7	1	1.3
-1 means low level and +1 means high level, and a center point was run to evaluate the linear and curvature effects of the variables			

Characterization

The bonding strength (BS) of test samples was determined by following precisely the conditions and methods described by the Chinese National Standard GB/T 9846 (2015). The size of the specimens was $25 \text{ mm} \times 12 \text{ mm}$ (L×W). Mechanical properties of the AAP were measured by a tensile testing machine (MTS Systems Corporation, Eden Prairie, MN, USA) with a rate of 10 mm/min (CMT6104; Shenzhen, China). The results were obtained from an average of 10 tested samples.

The analysis of the reaction mechanisms between the AP adhesive and plywood were performed using an X-ray diffraction analyzer (ESCALAB 250Xi, Thermo Fisher Scientific Inc., Waltham, MA, USA). The tested samples were prepared separately, drying the adhesive and the plywood sawdust at $175 \text{ }^\circ\text{C}$, after which they were sieved to a uniform particle mesh size of 0.15 mm .

The microstructures of the specimens were observed by scanning electron microscopy (SEM) at an acceleration voltage of 3 kV (Hitachi SU8010, Tokyo, Japan) Prior to testing, the samples for SEM were prepared by drying the gel portion of the dried solid adhesive in an oven at $175 \text{ }^\circ\text{C}$. Thereafter, a sliced portion of the dried solid adhesives was mounted on the test slide for a microscopic examination.

RESULTS AND DISCUSSION

Modeling and Optimization of APPs

Model fitting

The BBD was employed to develop a correlation between the preparation's plywood and bonding strength (Y) variables. The results obtained from all 17 tests are shown in Table 2.

The following second-order polynomial equation expresses the coefficients of the parameter variables (A, B, and C) for the response variable (Y) in terms of coded values:

$$Y = + 1.96 + 0.24A + 0.10B + 0.031C - 0.088AB + 0.0025AC + 0.025BC - 0.27A^2 - 0.13B^2 - 0.27C^2 \quad (1)$$

The significance of the fitted model for BS was evaluated by analysis of variance (ANOVA) (Table 3). Because the p-value of the model was less than 0.0001 and the F value was 98.841, the model had good fitness. The coefficient of determination (R^2) was defined as the ratio of the explained variation to the total variation and was a measurement of the degree of fitness. A small value of R^2 indicated poor relevance of the dependent variables in the model. With the variance analysis, the R^2 value of this model was determined as 0.992 and, when adjusted, was 0.982, which showed that the regression model could explain the system's exact behavior well (Chen *et al.* 2012).

Table 2. Experimental Designs and Response Values

Run No.	Coded Levels			Bonding Strength (MPa)	
	A (mL)	B (g)	C (mL)	Experimental	Predicted
1	150	5	0	84.87	85.09
2	180	5	+1	96.87	96.93
3	150	9	-1	83.68	87.27
4	180	9	-1	95.71	91.90
5	150	7	0	99.96	103.49
6	180	7	+1	83.52	83.23
7	150	7	+1	86.39	90.21
8	180	7	+1	98.65	95.06
9	165	5	-1	99.24	99.18
10	165	9	-1	94.67	94.96
11	165	5	0	95.35	95.13
12	165	9	0	97.54	94.01
13	165	7	0	116.82	117.62
14	165	7	0	117.16	117.62
15	165	7	0	117.31	117.62
16	165	7	0	118.53	117.62
17	165	7	0	118.3	117.62

In this case, the p-values of A, B, AB, A^2 , B^2 , and C^2 were all less than 0.05, indicating that these parameters were significant, whereas the AC and BC were not.

According to the sum of squares of the parameter variables, the effect of the parameters on the BS was as follows: temperature (A) > time (B) > pressure (C).

Table 3. Analysis of Variance for Regression Model for the Regression Equation

Source	Sum of Squares	Degree of Freedom	Mean Square	F Value	p-value
Model	1.359	9	0.151	98.841	< 0.0001*
A	0.461	1	0.461	301.599	< 0.0001
B	0.082	1	0.082	53.678	0.0002
C	0.008	1	0.008	5.113	0.058
AB	0.031	1	0.031	20.044	0.003
AC	0.00001	1	0.00001	0.016	0.902
BC	0.003	1	0.003	1.636	0.242
A ²	0.317	1	0.317	207.653	< 0.0001
B ²	0.073	1	0.073	48.018	0.0002
C ²	0.312	1	0.312	203.888	< 0.0001
Residual	0.011	7	0.002		
Lack of Fit	0.006	3	0.002	1.822	0.283
Pure error	0.005	4	0.001		
Cor. total	1.37	16			

p < 0.01 = highly significant; 0.01 < p < 0.05 = significant; p > 0.05 = insignificant

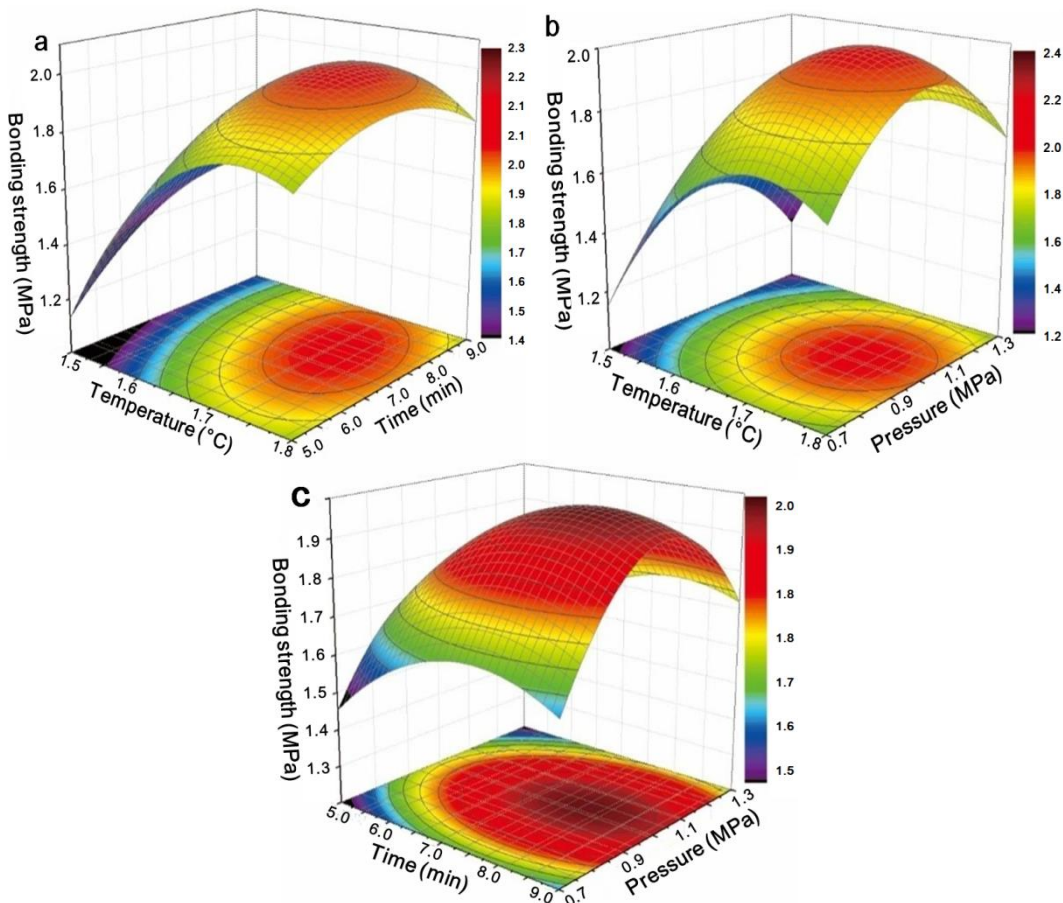


Fig. 1. Response surface plots for the maximum BS of plywood: (a) effects of temperature and time on the BS of plywood; (b) effects of temperature and pressure on the BS of plywood; (c) effects of time and pressure on the BS of plywood

Analysis of response surface and optimization

To further analyze the effect of the three factors on BS, the relationship between the parameters and response variable was illustrated in a 3D representation of the response surfaces (Fig. 1).

Figure 1a shows the effects of hot-pressing temperature and time on the BS of plywood. Hot-pressing time exhibited a weaker effect, whereas hot-pressing temperature represented a significant effect on BS. The maximal BS was determined when the temperature and time were 170 °C and 7 min, respectively. When the hot-pressing temperatures were 150 °C, the BS had the lowest value. This was because the AP adhesive was not fully cured at low temperature, which might harm the interface bonding between the veneer and adhesives. The BS decreased slightly with the increase of hot-pressing temperature after 170 °C because the partial hemicelluloses and lignin in fiber were under pyrolysis.

Figure 1b depicts that the interaction of hot-pressing temperature and relative pressure were relatively significant to BS. The effect of the temperature on BS followed a similar trend as that of the pressure. The hot-pressing temperature had a more obvious influence on BS, perhaps because the AP adhesive solidified completely at a certain temperature and pressure, the interface between wood fiber and adhesive was well bonded, and the mechanical strength was significantly improved.

Figure 1c shows that the plywood's BS increased quickly and then decreased slightly with the increase of the hot-press temperature. The result was elliptical, indicating significant interactive effects between the two independent variables on the BS of plywood. Therefore, the optimal conditions of pretreatment were obtained. They were a hot-pressing temperature of 171 °C, a time of 7.5 min, and a pressure of 1.0 MPa. Under these conditions, the model adequately reflected that the expected optimization was satisfactory and accurate.

Micromorphology of APP

As shown in Fig. 2, the distribution of AP adhesive film was continuous, which helped the formation of a good bonding interface. Figure 2b is a partial magnification of Fig. 2a. The AP adhesive coating can be seen on the surface of wood fiber. It played an important role in improving the corresponding mechanical properties.

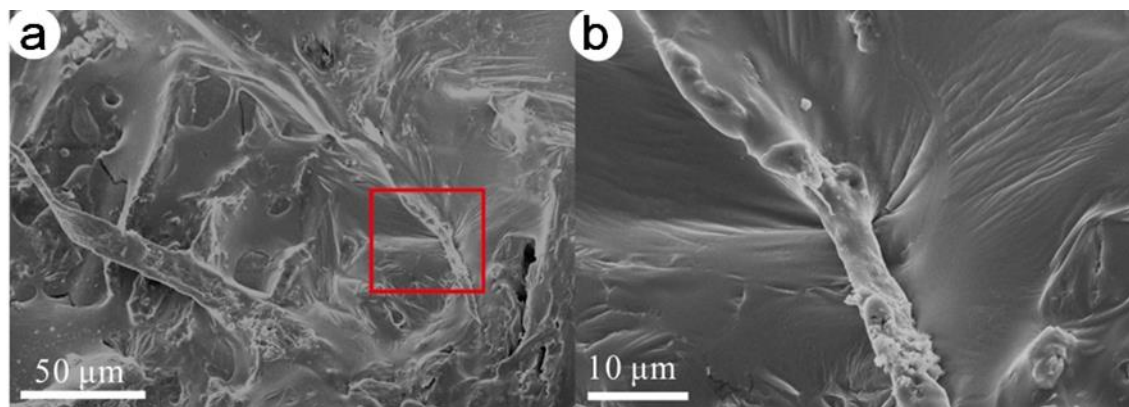


Fig. 2. (a) Micromorphology of plywood, and (b) partial magnification of detail from (a)

A layer of AP adhesive was wrapped on the wood fiber's outer surface, indicating that the AP adhesive had a good interface bond with the wood fiber. It thus improved the mechanical properties of the plywood.

X-ray Photoelectron Spectroscopy Analysis

To understand the relationship between AP adhesive and plywood, the AP adhesive and pure wood fiber were tested and analyzed using XPS. As shown in Fig. 3a, only C and O elements were seen in the XPS curve of pure wood fiber. In Fig. 3b, the main peak at position 284.6 eV belongs to C1 (C–C or C–H bond), the peak at position at 286.4 eV belongs to C2 (C–O bond), and the peak at position 288.5 eV belongs to C3 (C=O bond or O–C–O bond) in the XPS spectrum of the pure wood fiber (Xia *et al.* 2014). Among them, C1, C2, C3, and O/C accounted for 57%, 34.4%, 8.6%, and 0.29, respectively. In plywood, C1, C2, and C3 accounted for 81.4%, 12.7%, and 5.9%, respectively. Compared with pure wood fiber, the plywood peak prepared with AP adhesive decreased at the position of 286.4 eV. This decrease could have been caused by the hydrogen bond or chemical bond that formed between the wood fiber and the AP adhesive, which consumed some hydroxyl groups on the wood-fiber surface and reduced the proportional content of C2 and C3.

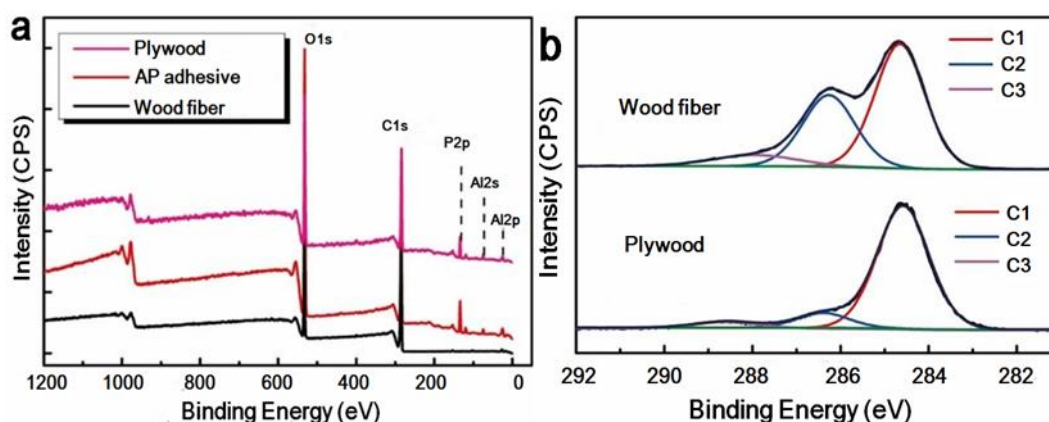


Fig. 3. Typical XPS spectra: (a) XPS spectrum of plywood, AP adhesive, and wood fiber, (b) C1, C2, and C3 of XPS spectrum of wood fiber and plywood

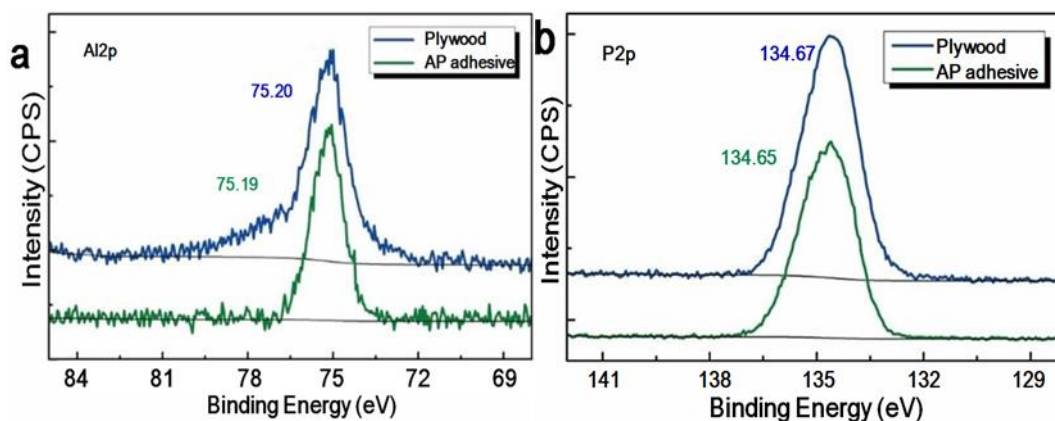


Fig. 4. Typical XPS of (a) Al_{2p} and (b) P_{2p} in AP adhesive and plywood

In the XPS curves corresponding to the AP adhesive, the characteristic peaks of P_{2p} and Al_{2p} were 134.65eV and 75.19eV, respectively (Fig. 4). In the plywood sample, the characteristic peaks of P_{2p} and Al_{2p} were 134.67eV and 75.20eV with 0.02 and 0.01eV higher than AP adhesive, respectively. The reason may be that the electronegativity values of the elements O, C, P, and Al were, respectively, 3.44, 2.55, 2.19, and 1.61. The electronegativity difference of O–C, O–P, and O–Al were 0.89, 1.25, and 1.83, respectively, which indicated that O–P and O–Al bonds could more easily obtain electronegativity than the O–C bond. The electron cloud densities of P and Al in plywood were lower than in the AP adhesive. If P–O–C and Al–O–C covalent bonds formed between AP adhesive and wood fiber, the peak binding energy of P_{2p} and Al_{2p} was lower in plywood than in the AP adhesive. However, as shown in Fig. 5, the peak position of P_{2p} and Al_{2p} was higher in the plywood than in the AP adhesive. Therefore, P–O–C and Al–O–C covalent bonds were not found between AP adhesive and wood fiber (Qiu and Li 2005; Chen *et al.* 2010; Hao *et al.* 2013; Xia *et al.* 2014).

It was conjectured that the reaction mechanism between the AP adhesive and wood fibers occurred as follows. Aluminum hydroxide reacted with phosphoric acid to form P–O–Al dimer with tetra- and hexa-coordination. In the reaction progress, the P–O–Al chain became longer, resulting in a linear or systematic polymer structure. The physical combination of AP adhesive and wood fiber during the hot-pressing process, which resulted in hydrogen bonds, mechanical binding force, and Van der Waals forces, gave the plywood certain mechanical strength. As the cellulose morphology changed and the hydrogen bonds were destroyed by pretreatment, the combination of the chemical and base materials were positively affected.

CONCLUSIONS

1. Response surface methodology was used to investigate hot-pressing temperature, time, and pressure, and a quadratic polynomial model was fit for this experiment.
2. After the optimization in Design Expert, the parameters of the plywood hot-pressing process were temperature, time, and pressure at 171 °C, 7.5 min, and 1.0 MPa, respectively. Under these conditions, the test results were repeatedly verified. The obtained adhesive strength of the plywood was 1.98 MPa, which was consistent with the calculated value of the equation, indicating the accuracy of the quadratic polynomial model.
3. The wood fiber was coated with a film of aluminophosphate (AP) adhesive. P–O–C and Al–O–C covalent bonds were not found between AP adhesive and wood fiber.

ACKNOWLEDGEMENTS

The authors are grateful for the financial support of the National Science and Technology Support Program (2008BADA9B01), the National Natural Science Foundation of China (NSFC) (30781982), the Scientific Research Foundation of Wuyi University (YJ201913), and Educational and Scientific Research Projects (science and technology) for Young and Middle-aged Teachers in the Fujian Province (JAT190785).

REFERENCES CITED

- Aghamohseni, B., Hassaninejad-Darzi, S. K., and Asadollahi-Baboli, M. (2019). "A new sensitive voltammetric determination of thymol based on MnY nanozeolite modified carbon paste electrode using response surface methodology," *Microchemical Journal* 145, 819-832. DOI: 10.1016/j.microc.2018.11.045
- Bahrami, H., Eslami, A., Nabizadeh, R., Mohseni-Bandpi, A., Asadi, A., and Sillanpää, M. (2018). "Degradation of trichloroethylene by sonophotolytic-activated persulfate processes: Optimization using response surface methodology," *Journal of Cleaner Production* 198, 1210-1218. DOI: 10.1016/j.jclepro.2018.07.100
- Bahrami, M., Amiri, M. J., and Bagheri, F. (2019). "Optimization of the lead removal from aqueous solution using two starch based adsorbents: Design of experiments using response surface methodology (RSM)," *Journal of Environmental Chemical Engineering* 7(1), Article ID 102793. DOI: 10.1016/j.jece.2018.11.038
- Balamurugan, K., Uthayakumar, M., Sankar, S., Hareesh, U. S., and Warriar, K. G. K. (2019). "Predicting correlations in abrasive waterjet cutting parameters of lanthanum phosphate/yttria composite by response surface methodology," *Measurement* 131, 309-318. DOI: 10.1016/j.measurement.2018.09.009
- Chen, Z. L., Fu, F., Ye, K. L., Wang, Q., and Zuo, T. Y. (2010). "Preparation of the SiO₂ gel/wood composites from TEOS sol with hydrolyzing," *Journal of Beijing University of Technology* 36(2), 250-254. DOI: 10.1016/j.optlastec.2018.06.026
- Chen, W., Wang, W. P., Zhang, H. S., and Huang, Q. (2012). "Optimization of ultrasonic-assisted extraction of water-soluble polysaccharides from *Boletus edulis* mycelia using response surface methodology," *Carbohydrate Polymers* 87(1), 614-619. DOI: 10.1016/j.carbpol.2011.08.029
- GB/T 9846 (2015). "Plywood for general use," Standardization Administration of China, Beijing, China.
- Hao, S. X., Wen, J., Yu, X. P., and Chu, W. (2013). "Effect of the surface oxygen groups on methane adsorption on coals," *Applied Surface Science* 264, 433-442. DOI: 10.1016/j.apsusc.2012.10.040
- Huang, Q., Zhao, X., Zheng, X., and Li, X. (2018). "Preparation and properties of silicon magnesium cement with bamboo particle board," *New Building Materials* 45(9), 25-29. DOI: 10.3969/j.issn.1001-702X.2018.09.006
- Jambo, S. A., Abdulla, R., Marbawi, H., and Gansau, J. A. (2019). "Response surface optimization of bioethanol production from third generation feedstock - *Eucheuma cottonii*," *Renewable Energy* 132, 1-10. DOI: 10.1016/j.renene.2018.07.133
- Liu, Z., Ma, L., Nie, N., Xiao, J., and Zhang, B. (2018). "Preparation and application of inorganic and environmentally friendly adhesive for straw-based panel," *China Forest Products Industry* 45(6), 47-51.
- Long, J. Q., Huang, W. H., Xiang, J. W., Guan, Q. Q., and Ma, Z. W. (2018). "Parameter optimization of laser welding of steel to Al with pre-placed metal powders using the Taguchi-response surface method," *Optics & Laser Technology* 108, 97-106.
- Majdi, H., Esfahani, J. A., and Mohebbi, M. (2019). "Optimization of convective drying by response surface methodology," *Computers and Electronics in Agriculture* 156, 574-584. DOI: 10.1016/j.compag.2018.12.021

- Mei, C. T., Han, G. P., and Wu, Z. K. (2012). *Particleboard Manufacturing*, China Forestry Press, Beijing, China.
- Mestry, A. P., Mujumdar, A. S., and Thorat, B. N. (2011). "Optimization of spray drying of an innovative functional food: Fermented mixed juice of carrot and watermelon," *Drying Technology* 29(10), 1121-1131. DOI: 10.1080/07373937.2011.566968
- Nayak, M. G., and Vyas, A. P. (2019). "Optimization of microwave-assisted biodiesel production from papaya oil using response surface methodology," *Renewable Energy* 138, 18-28. DOI: 10.1016/j.renene.2019.01.054
- Ooi, T. Y., Yong, E. L., Din, M. F. M., Rezaia, S., Aminudin, E., Chelliapan, S., Rahman, A. A., and Park, J. (2018). "Optimization of aluminium recovery from water treatment sludge using response surface methodology," *Journal of Environmental Management* 228, 13-19. DOI: 10.1016/j.jenvman.2018.09.008
- Pérez-Francisco, J. M., Cerecero-Enríquez, R., Andrade-González, I., Ragazzo-Sánchez, J. A., and Luna-Solano, G. (2008). "Optimization of vegetal pear drying using response surface methodology," *Drying Technology* 26(11), 1401-1405. DOI: 10.1080/07373930802333601
- Qiu, J., and Li, J. (2005). "Preparation of wood-silica aerogels composites by supercritical drying technique and its nano-structure," *Journal of Northeast Forestry University* 33(3), 3-4.
- Sharma, D., Yadav, K. D., and Kumar, S. (2018). "Biotransformation of flower waste composting: Optimization of waste combinations using response surface methodology," *Bioresource Technology* 270, 198-207. DOI: 10.1016/j.biortech.2018.09.036
- Song, H. W., Dan, J. Q., Li, J. L., Du, J., Xiao, J. F., and Xu, J. F. (2019). "Experimental study on the cutting force during laser-assisted machining of fused silica based on the Taguchi method and response surface methodology," *Journal of Manufacturing Processes* 38, 9-20. DOI: 10.1016/j.jmapro.2018.12.038
- Sulaiman, N. S., Hashim, R., Mohamad, A. H. M., Danish, M., and Sulaiman, O. (2018). "Optimization of activated carbon preparation from cassava stem using response surface methodology on surface area and yield," *Journal of Cleaner Production* 198, 1422-1430. DOI: 10.1016/j.jclepro.2018.07.061
- Šumić, Z., Vakula, A., Tepić, A., Čakarević, J., Vitas, J., and Pavlić, B. (2016). "Modeling and optimization of red currants vacuum drying process by response surface methodology (RSM)," *Food Chemistry* 203, 465-475. DOI: 10.1016/j.foodchem.2016.02.109
- Sun, H. J., Sun, L. P., and Jiang, B. (2014). "Study on fuzzy controlling of hot pressing time of medium-density fiberboard," *Wood Processing Machinery* 25(2), 4-6.
- Wang, Y. F., and Wang, C. G. (2005). "The application of response surface methodology," *Journal of the Central University for Nationalities (Natural Sciences Edition)* 14(3), 236-240.
- Xia, W. C., Yang, J. G., and Liang, C. (2014). "Investigation of changes in surface properties of bituminous coal during natural weathering processes by XPS and SEM," *Applied Surface Science* 293, 293-298. DOI: 10.1016/j.apsusc.2013.12.151
- Zhu, X. D., Wu, Y. Q., Tian, C. H., Yang, J. M., and Zhang, X. L. (2015). "Study on the preparation process and properties of wheat straw board cemented with inorganic glue," *China Forest Products Industry* 42(6), 18-22.

Zuo, Y. F., Wu, Y. Q., Lyu, J. X., Liu, Y., and Li, X. G. (2016). “Effect of process parameters on the properties of rice straw board with inorganic adhesive,” *China Forestry Science and Technology* 1(4), 25-32. DOI: 10.13360/j.issn.2096-1359.2016.04.004

Article submitted: August 17, 2020; Peer review completed: November 28, 2020; Revised version received and accepted: January 19, 2021; Published: January 21, 2021.
DOI: 10.15376/biores.16.1.1702-1712